

Impact of a liquid mass on a perfectly plastic solid

By P. A. LUSH

Department of Mechanical Engineering, The City University, London

(Received 1 July 1982 and in revised form 31 March 1983)

The use of steady, normal and oblique shock configurations is explored in calculating the pressure and deformation produced by the impact of a liquid mass on a plane solid surface. Since pressures generated are very large, the change in bulk modulus of the liquid (water) is accounted for by using an equation of state following Field, Lesser & Davies (1979). The impact of a plane-ended liquid mass is analysed using a normal shock for the cases of a rigid surface and a perfectly plastic surface. For the former, it is found that pressures somewhat in excess of the 'water-hammer' pressure of linear acoustic theory are predicted, and for the latter there is a critical impact velocity below which no deformation occurs. Above this velocity the surface deforms at a constant rate, producing a pit with maximum depth at the centre.

If the liquid mass is wedge-shaped then an oblique shock is formed, which is attached to the contact point provided that the impact Mach number is large enough, as originally shown by Heymann (1969). Pressure and deformation velocity can again be calculated for the cases of rigid and perfectly plastic surfaces respectively. For a rigid surface it is confirmed that pressures considerably in excess of the plane-ended case are produced at shock detachment. For the plastic surface, it is found that there is no critical impact velocity and deformation can occur at any velocity as shock detachment is approached. For a cylindrical liquid mass with a conical tip, the pit produced again has maximum depth at the centre, but with a considerably increased value. The possible use of these models for pitting caused by microjets associated with cavitation bubbles and by impact of liquid drops is discussed.

1. Introduction

In this paper the use of steady two-dimensional shock configurations is explored further for the purpose of estimating the pressure and deformation produced by the impact of a liquid mass on a plane surface. Some knowledge of these quantities is desirable in understanding the mechanism of erosion produced by a cavitating flow or by impacting rain drops. Previously the impact of plane-ended or spherical liquid masses on a rigid surface has received considerable attention and pressures of the same order as the water-hammer pressure, calculated according to linear acoustic theory, have been both predicted and observed experimentally (for up-to-date summary see Brunton & Rochester 1979).

The problem of the impact of spherical drops was advanced by Heymann (1969), who considered the case of a wedge-shaped liquid mass impinging on a rigid surface; since the angle between the liquid and solid surfaces is constant, the contact point moves at a constant velocity and problem can be tackled as a steady flow through a plane oblique wave, which is at rest in a reference frame moving with the contact point. Heymann showed that a maximum pressure of around three times the 'water-hammer' pressure was produced when the shock became detached from the

contact point. More recently, Field, Lesser & Davies (1979) have reworked Heymann's analysis using an equation of state for the liquid (water) which allows more accurately for the increase in density and sound speed with pressure.

Also recently, the present author (Lush 1979) has adapted the model originally used by Bowden & Brunton (1961), i.e. the impact of a plane-ended liquid cylinder upon a rigid surface, to calculate the deformation of a perfectly plastic surface under a similar impact. The velocity of deformation is determined from the momentum equation assuming that the pressure is constant and equal to the stress required for plastic flow. Liquid compressibility is allowed for by using the same equation as Field *et al.* When account is taken of the propagation of a pressure release wave towards the centre of the cylinder, the maximum depth of penetration in the centre can be calculated. This paper seeks to combine these two ideas, namely the use of a wedge-shaped liquid mass and perfectly plastic deformation, in order to find the deformation produced by conically ended liquid jets in a perfectly plastic medium. It is suggested that this model might be applicable to the case of microjets associated with cavitation bubbles. The curvature of the liquid surface in the case of droplets means that the contact point is decelerated as the impact proceeds and the method does not therefore strictly apply, although it may be used to give an indication of the deformation. Lesser (1979) has given a solution for the spherical droplet which allows the pressure distribution under the droplet to be calculated for the case of a rigid solid and he has recently (1981) extended this solution to the case of impact on an elastic medium. Therefore it would seem that consideration of a perfectly plastic medium is timely and this is the main purpose of this paper, though the case of a rigid medium is considered for completeness.

2. Impact of a plane-ended liquid mass

We consider first the impact of a plane-ended liquid mass on a plane solid surface. The direction of motion of the liquid mass is at right angles to the surface, the plane end being parallel to the surface. When the liquid strikes this surface a normal shock wave is propagated against the liquid stream, and behind the shock the liquid velocity is reduced and the pressure increased. The exact relation between them is determined by the response of the surface, which is initially assumed to be quite general. Assuming, for the moment, that the liquid mass is infinitely wide, the problem can be analysed in one-dimensional terms and is most simply done in a reference frame moving with the shock, since in this frame the flow is steady (figure 1). If the velocity of the liquid is initially v , the velocity behind the shock is u and the velocity of the shock wave is $-c$, which is not necessarily equal to the sound speed, then, in the steady flow reference frame, the equation of continuity is

$$\rho_0(v+c) = \rho(u+c), \quad (1)$$

where ρ_0 is the ambient density of the liquid and ρ that behind the shock. If the pressure behind the shock is p , then by conservation of momentum it can be shown that

$$p-p_0 = \rho_0(v+c)(v-u), \quad (2)$$

where p_0 is the ambient pressure. Equations (1) and (2) can be solved provided that the relation between pressure and density is known. It is usual to assume that the relation for water has the form

$$\frac{p+B}{p_0+B} = \left(\frac{\rho}{\rho_0}\right)^n, \quad (3)$$

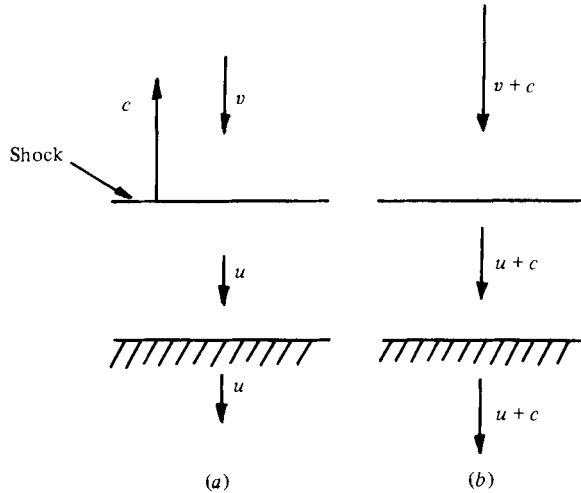


FIGURE 1. Normal-shock configuration for (a) unsteady and (b) steady reference frames.

where $n \approx 7$ and $B \approx 300$ MPa. Strictly (3) applies only to isentropic changes, but can be applied with reasonable accuracy in general since n is independent of entropy and B and ρ_0 are only slowly varying functions of entropy (see Batchelor 1967). For small values of the change in velocity, $v - u$, the quantity $\rho_0(v + c)$ in (2) reduces to the familiar acoustic form $\rho_0 c_0$, where c_0 is the ambient sound speed. Since for water ρ_0 and c_0 are approximately 1000 kg/m^3 and 1450 m/s respectively, for all but the smallest velocities, i.e. greater than about 10 m/s , the ambient pressure (assumed to be 0.1 MPa) can be neglected in both (2) and (3). With this approximation the relation between pressure p and velocity difference $v - u$ is

$$v - u = \left[\frac{p}{\rho_0} \left(1 - \left(1 + \frac{p}{B} \right)^{-1/n} \right) \right]^{\frac{1}{2}}. \tag{4}$$

If the impact is with a rigid surface, then u is zero, and (4) gives the impact pressure in terms of the impact velocity (figure 2). It can be seen that the pressure generated increases considerably above that given by the acoustic approximation, i.e. $\rho_0 c_0 v$. If the surface is elastic then a relation between p and u is known in terms of the elastic modulus of the material, and together with (4) can be used to solve for the pressure. However, in the present work we are interested in a surface which responds as a rigid solid until a certain compressive stress is reached and then behaves as a perfectly plastic solid, for which the stress will remain constant, equal to p_Y , say. In this case (4) can be rewritten to give the velocity of deformation u in terms of the impact velocity v and the stress to produce plastic flow, p_Y , i.e.

$$u = v - v_0, \tag{5a}$$

where

$$v_0 = \left[\frac{p_Y}{\rho_0} \left(1 - \left(1 + \frac{p_Y}{B} \right)^{-1/n} \right) \right]^{\frac{1}{2}}. \tag{5b}$$

It is apparent that the impact velocity must exceed a certain critical value v_0 before any plastic deformation can occur. The relation (5b) is effectively given in figure 2.

Hitherto we have assumed that the liquid mass is infinite in width; but in reality

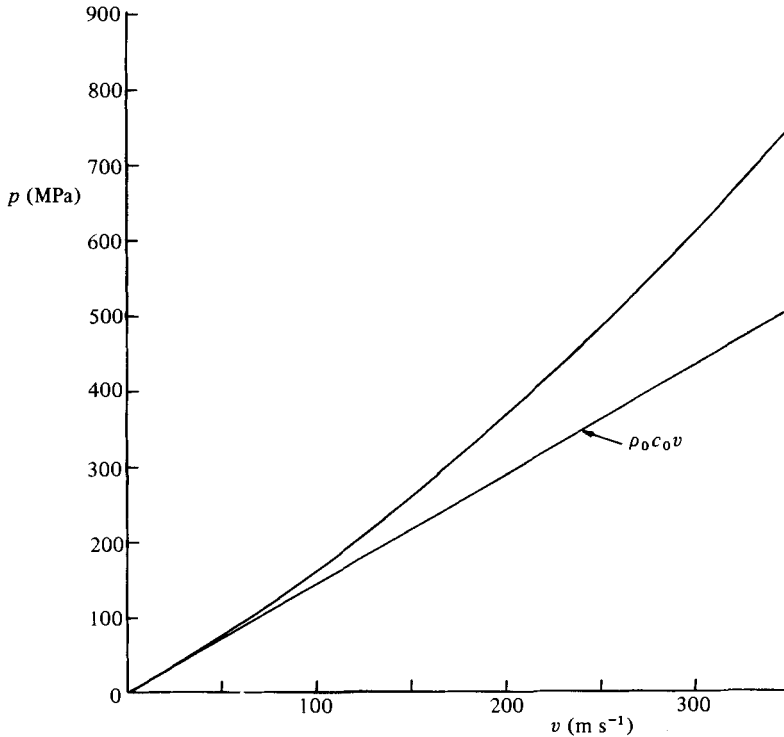


FIGURE 2. Pressure p generated by impact of plane-ended liquid mass at velocity v on a rigid surface.

this will not be the case, and, as soon as the liquid strikes the surface, a release wave will propagate from the edge of the liquid mass towards the impact centre at the ambient sound speed. Assuming the liquid mass to be a cylinder of radius a , the pressure at the centre will decrease after a time a/c_0 from the value given by (4) to the stagnation pressure $\frac{1}{2}\rho_0 v^2$, which will be an order of magnitude smaller unless exceptionally high impact velocities are encountered.

For the perfectly plastic material, it is assumed that at any instant the situation is the same as that for a two-dimensional flat punch penetrating the surface and producing large-scale deformation (figure 3). This problem can be solved by using slipline theory (see Tabor 1951), which shows that the stress P normal to the surface under the punch is given by

$$P = 2k(1 + \frac{1}{2}\pi) \quad (6)$$

and the transverse stress Q by

$$Q = 2k \frac{\pi}{2} \quad (7)$$

where k is the critical value of the maximum shear stress at which plastic flow occurs. Depending on the criterion for plastic flow which is adopted, the value of $2k$ is either 1.0 or $2/\sqrt{3}$ times the uniaxial yield stress Y . It is usually reckoned that the normal stress required for full-scale plastic flow, using (6), is given approximately by

$$P = 3Y (= p_Y). \quad (8)$$

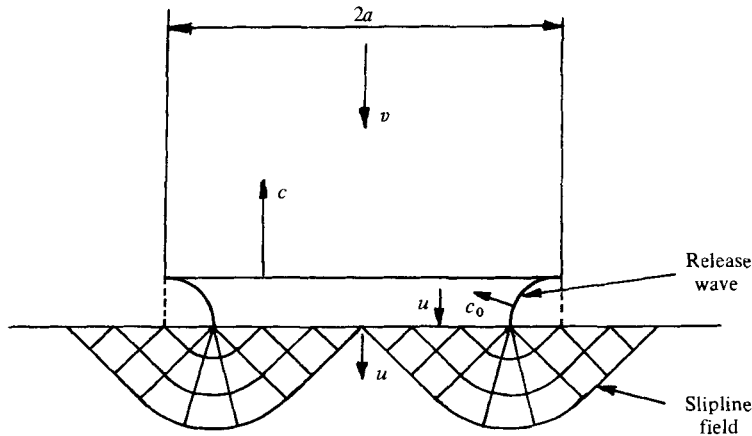


FIGURE 3. Impact of plane-ended liquid mass showing slipline field in plastic region.

Once the material is plastic, the velocity of deformation is determined by the external conditions and can be obtained from the above analysis (equation (5)). The amount of deformation at any point can then be estimated by taking into account the velocity components at the surface of the plastic region, both normal and parallel to the surface, and the time available for movement to occur. However, we can avoid this complication by considering only the centre of the impact, where the only motion will be normal to the surface and the depth of penetration will be a maximum. If it is assumed that plastic flow is established immediately, and that it ceases as soon as the release wave reaches the centre, the time available for deformation will be simply equal to the time taken for the wave to travel across the radius of the liquid cylinder; i.e. a/c_0 , assuming that it travels at the ambient liquid sound speed. Since the deformation velocity given by (5) is constant, the depth d of penetration at the centre is given simply by the product of the velocity u from (5) and the time available, i.e. by

$$\frac{d}{a} = \frac{v - v_0}{c_0}. \quad (9)$$

We are here ignoring the correction required to allow for the time delay before plastic flow can be established (see Lush 1979). Immediately after the impact, the stress field in the central region is the same as for an infinitely wide liquid mass. Release waves from the edge of the liquid propagate in both the solid and the liquid, the former being considerably faster. After the release wave in the solid has reached the centre, full-scale plastic flow as for a flat punch can be established, and this does not cease until the liquid release wave reaches the centre. The correction mentioned above may be omitted in principle if we idealize the material as rigid-perfectly plastic, in which case the effect of the impact is communicated instantaneously to the material and there will be no plastic wave. In reality there will be both elastic and plastic waves propagating in the material. Further consideration of this point is deferred until the end of §4.

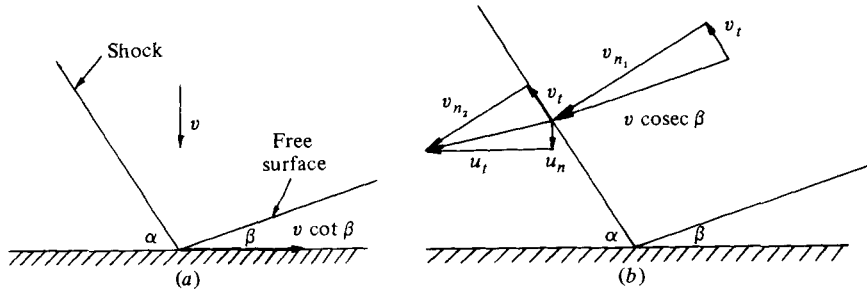


FIGURE 4. Oblique shock configuration for (a) unsteady and (b) steady reference frames.

3. Impact of wedge-shaped liquid mass

3.1. General equations

We now consider the normal impact at velocity v of a wedge-shaped liquid mass upon a plane surface, in which the front face of the wedge is plane but makes an angle β with the surface (figure 4). This is the configuration studied by Heymann and by Field *et al.* for impact on rigid surfaces, but the following development is for general surfaces. As pointed out originally by Bowden & Field (1964), if the angle β is sufficiently small the contact point moves supersonically and an oblique shock forms at the contact point, making an angle α , say, to the original surface. For the wedge-shaped configuration both the velocity of the contact point and the shock and contact angles, α and β respectively, remain constant and therefore the problem can be analysed as a steady flow in a reference frame in which the contact point is at rest. In this reference frame which is moving parallel to the surface at velocity $v \cot \beta$, the liquid approaches the surface at an angle β and with a velocity $v \operatorname{cosec} \beta$. Behind the oblique shock, the liquid changes direction and has a velocity u , say, which can conveniently be resolved into components normal and parallel to the original surface, u_n and u_t respectively.

The shock problem is analysed by resolving the velocity upstream of the shock into components normal and parallel to the shock, v_{n_1} and v_t , i.e.

$$v_{n_1} = v \operatorname{cosec} \beta \sin (\alpha + \beta), \quad v_t = v \operatorname{cosec} \beta \cos (\alpha + \beta). \quad (10)$$

On passing through the shock, the normal component is changed to v_{n_2} , but the transverse component v_t is unchanged. The components normal and parallel to the original surface are therefore given by

$$u_n = v_{n_2} \cos \alpha - v_t \sin \alpha, \quad u_t = v_{n_2} \sin \alpha + v_t \cos \alpha. \quad (11)$$

The equations of continuity and conservation of momentum are used to relate the normal velocity components to the pressure and density behind the shock, i.e.

$$\rho_0 v_{n_1} = \rho v_{n_2}, \quad (12)$$

$$p - p_0 = \rho_0 v_{n_1} (v_{n_1} - v_{n_2}). \quad (13)$$

Making use of the equation of state (3) and the relations (10), and also neglecting the ambient pressure as before, it can be shown that the pressure is given implicitly by

$$p = \rho_0 v^2 \operatorname{cosec}^2 \beta \sin^2 (\alpha + \beta) \left[1 - \left(1 + \frac{p}{B} \right)^{-1/n} \right]. \quad (14)$$

Using (11), the normal velocity is given by

$$u_n = v \operatorname{cosec} \beta \sin(\alpha + \beta) \cos \alpha \left[\left(1 + \frac{p}{B} \right)^{-1/n} - \frac{\tan \alpha}{\tan(\alpha + \beta)} \right]. \quad (15)$$

These equations will in general give either two solutions, corresponding to the weak and strong shock cases, or no solution. The transition between the two regions gives the locus where the oblique shock just becomes detached from the contact point. In this case, since the front face of the liquid wedge is a free surface, a release wave will propagate into the liquid, thus allowing the liquid to flow laterally and the pressure to decrease to ambient. The condition for shock detachment is found in general by simultaneously equating the differentials dv and $d\beta$ to zero. Then the boundary condition of either rigid surface i.e. $u_n = 0$ or perfectly plastic surface, $dp = 0$, allows an expression to be deduced.

3.2. Rigid surface

In the case of a rigid surface, the normal velocity component is zero, and (15) becomes

$$1 + \frac{p}{B} = \left[\frac{\tan(\alpha + \beta)}{\tan \alpha} \right]^n. \quad (16)$$

On incorporating this into (14), it can be shown that this equation reduces to

$$p = \rho_0 v^2 \left(1 + \frac{\tan \alpha}{\tan \beta} \right). \quad (17)$$

For given values of impact velocity v and wedge angle β it is possible to solve (16) and (17) for the impact pressure p and the shock angle α . Since α is of secondary interest, the solution is shown graphically (figure 5) as the variation of impact pressure with impact velocity v and angle β . When β is zero these equations are singular, but it can be shown that, if the shock angle α also tends to zero, (16) and (17) reduce to (4), i.e. the plane-ended case. The curve derived from (4) is also shown in figure 5.

The curves are truncated at shock detachment, showing only the weak-shock solution; this is taken to be the appropriate one because it agrees with the plane-ended case as β tends to zero. The shock-detachment condition is found by differentiating (16) and (17) and putting dv and $d\beta$ equal to zero, from which it may be deduced that

$$\frac{\rho_0 v^2}{nB} = \left[\frac{\tan(\alpha + \beta)}{\tan \alpha} \right]^n \frac{\tan \beta}{\tan \alpha} \left[\frac{\sin 2\alpha}{\sin 2(\alpha + \beta)} - 1 \right]. \quad (18)$$

When the left-hand side of (18), which is effectively the square of the impact Mach number, becomes less than the right-hand side, the shock will become detached.

The locus of shock detachment is approximately linear, and it is found that the value of $p/\rho_0 c_0 v$ is always greater than the minimum value of approximately 2.82, which occurs at the impact velocity of about 150 m/s, corresponding to a Mach number of 0.1. This result agrees well with those given by Heymann and by Field *et al.*, and indicates that the impact pressure is given to a good approximation by

$$p = 2.9 \rho_0 c_0 v, \quad (19)$$

with no more than a 3% error between the impact velocities of 70 and 340 m/s.

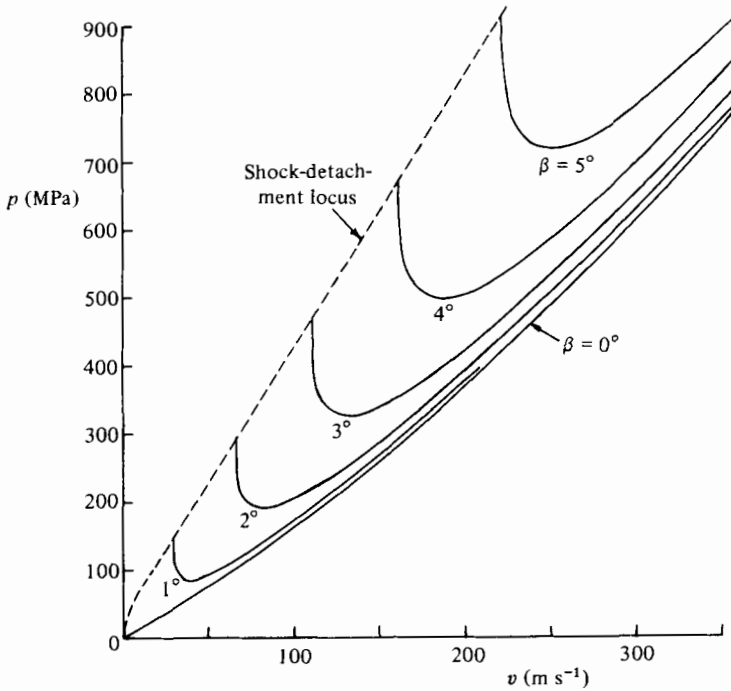


FIGURE 5. Pressure p generated by impact of wedge-shaped liquid mass at velocity v on a rigid surface.

3.3. Perfectly plastic surface

We turn now to the case of a perfectly plastic surface, for which the pressure will remain constant but the velocity normal to the original surface will be non-zero in general. The results (14) and (15) can be rewritten in terms of p_Y , the stress for plastic flow, as follows:

$$v \operatorname{cosec} \beta \sin (\alpha + \beta) = \left[\frac{p_Y / \rho_0}{1 - (1 + p_Y / B)^{-1/n}} \right]^{\frac{1}{2}}, \quad (20)$$

$$u_n = v \operatorname{cosec} \beta \sin (\alpha + \beta) \cos \alpha \left[\left(1 + \frac{p_Y}{B} \right)^{-1/n} - \frac{\tan \alpha}{\tan (\alpha + \beta)} \right]. \quad (21)$$

These equations may be solved for the shock angle α and normal velocity u_n in terms of wedge angle β , impact velocity v and plastic flow stress p_Y subject to the condition that u_n is positive, since negative values will be physically impossible. Since once again the shock angle is of secondary importance, the result, shown in figure 6, gives only the variation of normal velocity with impact velocity and wedge angle; the plastic flow stress is chosen as 400 MPa, which is a typical figure for 99% pure aluminium. In the limit of both α and β tending to zero, it can be shown that (20) and (21) reduce to the result for the plane-ended case (5).

The shock-detachment condition may be deduced on differentiating (20) and putting dv and $d\beta$ equal to zero to obtain

$$\cos (\alpha + \beta) = 0, \quad (22)$$

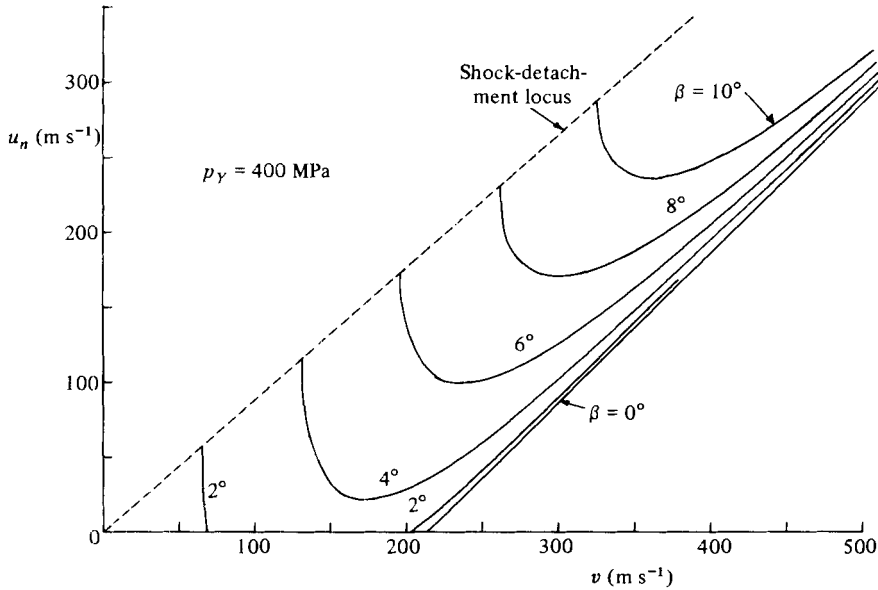


FIGURE 6. Deformation velocity u_n produced by impact of wedge-shaped liquid mass at velocity v on a perfectly plastic surface for $p_Y = 400$ MPa.

from which it follows that $\alpha + \beta$ must be equal to 90° . The shock remains attached to the contact point provided that $\alpha + \beta$ is less than 90° . At shock detachment it follows immediately from (20) and (21) that

$$v = \sin \beta \left[\frac{p_Y / \rho_0}{1 - (1 + p_Y / B)^{-1/n}} \right]^{\frac{1}{2}}, \quad (23)$$

$$u_n = v \left(1 + \frac{p_Y}{B} \right)^{-1/n}. \quad (24)$$

From (23) it can be seen that the critical value of β is approximately linearly proportional to v , for small values of β , and from (24) it follows that the shock-detachment locus, shown in figure 6, is a straight line passing through the origin with a slope dependent on the plastic flow stress.

If we now assume that the impact velocity and wedge angle are such that shock detachment does not occur, and also adopt the same model of large-scale plastic flow as in the plane-ended case, then the material behind the shock deforms at a constant velocity normal to the original surface, both while the shock remains attached to the contact point (figure 7) and during the passage of release waves (similar to figure 3). The amount of deformation will again depend on the time available before release waves cause the plastic flow to cease. It is possible that the velocity component parallel to the surface behind the shock will cause a substantial transverse shear stress, which will alter the normal stress required to maintain plastic flow; see (6) and (7). It is normally assumed that such viscous stresses are negligible (see e.g. Heymann 1969), but the validity of this assumption is not obvious, since viscous layers will be very thin giving rise to large velocity gradients. The transverse velocity behind the shock relative to the surface is typically an order of magnitude smaller than that of the contact point itself, i.e. of order 100 m/s; assuming that the time available for

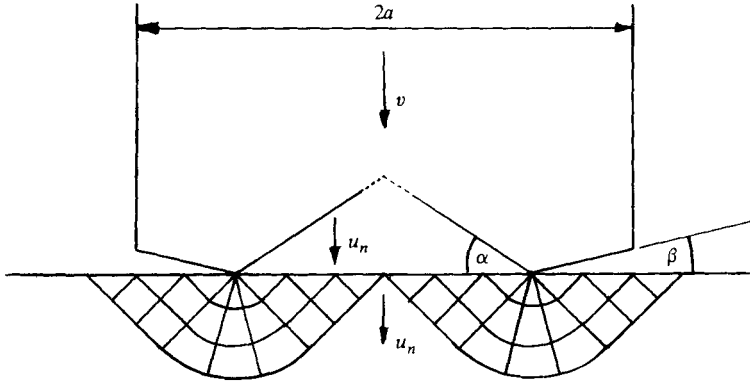


FIGURE 7. Impact of wedge-shaped liquid mass showing slipline field in plastic region.

the viscous layer to grow is of order $1 \mu\text{s}$, then, for water at normal temperature, the viscous-layer thickness will be of order $1 \mu\text{m}$, giving a shear stress of order 0.1 MPa . This is a large stress by normal standards, but in this context it is quite negligible since the stresses generated in the solid are of order 100 MPa .

We consider a cylindrical liquid mass of radius a with a conical tip; the inclined face makes an angle β with the surface which is normal to the direction of motion. Again, considering only the centre of the impact, where the depth of penetration will be a maximum, the time for deformation will be equal to the sum of the time required for the contact point to travel to the edge of the liquid jet and the time taken for the release wave to travel back, i.e.

$$a \left(\frac{1}{v \cot \beta} + \frac{1}{c_0} \right). \quad (25)$$

The depth of penetration is therefore found by taking the product of the deformation velocity u_n and the time available, and hence the maximum depth is given by

$$\frac{d}{a} = \frac{u_n}{c_0} \left(\frac{c_0 \tan \beta}{v} + 1 \right). \quad (26)$$

Because of the finite time required for the contact point to travel across the jet, the time available will in general be greater than that for the plane-ended jet. Coupled with the result that the deformation velocity is also greater (figure 6), the maximum depth of penetration will be considerably in excess of the plane-ended case. Strictly this model can only apply if the velocity of the contact point is less than the bulk sound speed in the solid material. Only in this case can the full-scale plastic deformation be established instantaneously around the point of contact. If the contact point is supersonic with respect to the solid, then the material behind the initial wave will be in a state of incipient plastic flow until a release wave has propagated in the solid, after which the full-scale plastic deformation can take place. The critical impact velocity is found by equating $v \cot \beta$ to the bulk sound speed in the solid material. Taking this to be 6300 m/s , i.e. for aluminium, the critical velocity ranges from about 110 m/s at $\beta = 1^\circ$ to 550 m/s at $\beta = 5^\circ$.

On combining (20) and (21) with (26), the maximum depth of pit expressed as d/a can be calculated as a function of impact velocity for various values of β (figure 8).

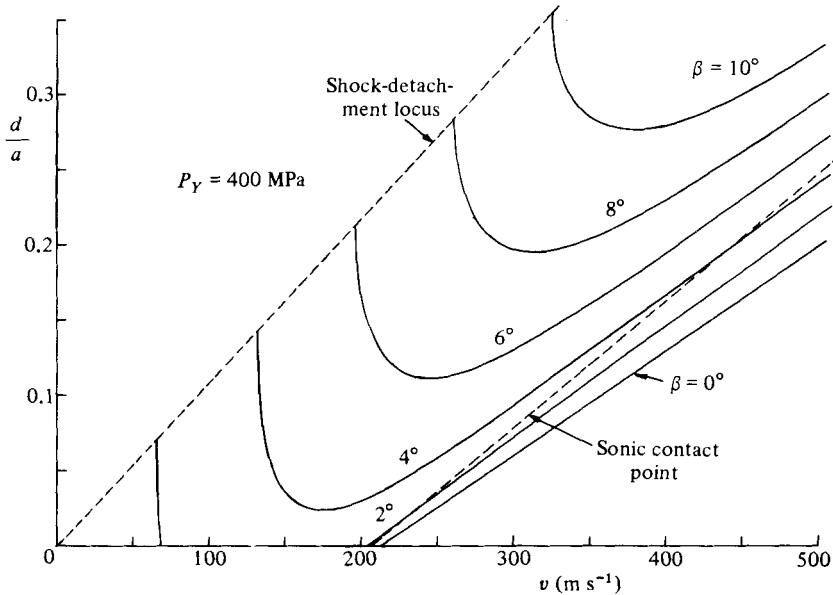


FIGURE 8. Maximum depth d produced by impact of wedge-shaped liquid mass at velocity v on a perfectly plastic surface.

By applying the condition (22), the shock detachment locus also shown in the figure is given by

$$\frac{d}{a} = \frac{v}{c_0} \left(1 + \frac{p_Y}{B}\right)^{-1/n} \left\{ \sec \beta \left[\frac{(1 - (1 + p_Y/B)^{-1/n})^{3/2}}{p_Y/nB} \right] + 1 \right\}, \quad (27)$$

which is a straight one passing through the origin if β is small.

The results given by figures 6 and 8 are for a plastic flow stress of 400 MPa. If other values are considered it is found that the overall picture is unchanged but the details are different. In general, as the plastic flow stress is increased, the critical impact velocity required to maintain the attached shock configuration is also increased, and the deformation velocity and maximum depth at a given impact velocity are decreased (figure 9). It is interesting to note that at a constant wedge angle the maximum depth varies only slowly with impact velocity, since the reduction in deformation velocity is almost compensated by the increase in time available.

4. Discussion

For the normal impact of a plane-ended cylinder of water on a rigid surface, it can be seen that the stress produced is given quite accurately by the 'water-hammer' expression for impact velocities below about 100 m/s. At higher velocities, the change in bulk modulus of the liquid causes a substantially higher stress to be produced. For impact with a surface producing plastic flow at a constant stress, there is a critical minimum or threshold impact velocity whose value is dependent on the material, and below which no permanent deformation occurs; above this velocity any change in impact velocity produces an equal change in deformation velocity. On taking into account the time available for deformation, the maximum depth of penetration can be calculated. Although the maximum depth is directly proportional to the difference between the impact velocity and the threshold impact velocity, the variation with

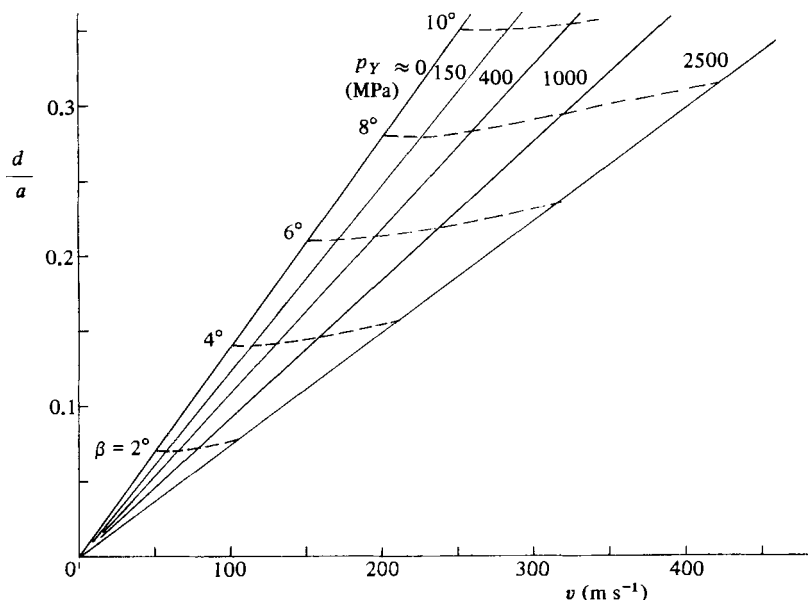


FIGURE 9. Maximum depth d produced at shock detachment by impact of wedge-shaped liquid mass at velocity v on a perfectly plastic surface.

impact velocity is essentially nonlinear because of this threshold velocity. Quite large plastic strains, far in excess of the elastic limit, can be produced according to this model. The value of the threshold velocity depends directly on the stress required for plastic flow. Because of the similarity of the pitting process to an indentation test to measure hardness, the stress required to produce plastic flow is the same as that given by a hardness test, which appears to provide a convenient way of estimating it for different materials. Because of the large rates of strain involved in impact damage, it would be more appropriate to use dynamic hardness, as measured by a falling-ball scleroscope. The figure quoted above for 99% pure aluminium was taken from a diamond-pyramid test, which gave a value of 40, i.e. approximately 400 MPa; a falling-ball test on the same material gives a stress in the region of 1300 MPa, larger by a factor of more than three. Therefore, for the plane-ended impact, even quite soft materials like aluminium will require a very large threshold velocity, in excess of 500 m/s, to produce plastic deformation.

If the front face of the impacting liquid is inclined at a small angle to the surface, the stress produced on a rigid surface can be increased quite considerably. The larger the angle, the higher is the stress produced, but the velocity has to be high enough to ensure that the oblique shock remains attached to the contact point, thus delaying the propagation of the release wave. In fact there is a locus of shock-detachment points which may be regarded as an upper limit of impact stress produced given by (19); just as the plane-ended case, i.e. zero contact angle, can be regarded as a lower limit, given by (4) with $u = 0$.

For the plastic surface impacted by liquid inclined at a small angle to the surface, it is found that the deformation velocity and maximum depth are likewise increased compared with the plane-ended case. There is now no threshold impact velocity, but there is an upper limit to the deformation given by the shock-detachment locus, (24) and (27). Thus the main effect of having a wedge-shaped liquid mass is to allow

deformation to occur at impact velocities right down to zero. The effect of hardness, i.e. p_Y , is simply to modify the amount of deformation.

It should be noted that we have deliberately restricted the calculation to the maximum depth of pit, i.e. at the centre, because finding the exact pit profile requires a more detailed treatment of the plastic flow; in particular, allowance must be made for the displacement of material outside the zone of contact, which is in a different direction to displacement within the zone.

If this model is to be applied to the pitting produced by the microjet associated with cavitation-bubble collapse, it is necessary to assume that the cavity is in contact with the surface and that the microjet has a conical tip with a semiangle almost as large as 90° and a radius considerably smaller than the initial cavity radius. The calculations of Plesset & Chapman (1971) indicate that the microjet radius is about one-tenth of the initial cavity radius and also that microjet velocities are very high, being given by $12.8(\Delta p/\rho_0)^{1/2}$, where Δp is the pressure difference tending to collapse the cavity. For Δp between 0.1 and 1 MPa, the microjet velocity will be between 130 and 400 m/s approximately, assuming that the fluid is water, and the shock will remain attached provided that the wedge angle is not greater than about 4° and 12° respectively for a material of hardness corresponding to 400 MPa, from (23). For softer materials these angles are increased somewhat and for harder materials they are reduced. Plesset & Chapman also show that the microjet tip is approximately conical with a semiangle of about 55° , corresponding to a wedge angle of 35° ; this value is much too large for the shock wave to be produced at velocities as low as 400 m/s. However, if we simply postulate that some microjet impacts will have sufficiently small wedge angles for the shock to remain attached, then the largest pit depths will be produced at shock detachment. Since this locus passes through the origin, damage can occur at any velocity. This contrasts with the plane-ended case, which predicts a threshold velocity below which no damage occurs.

Similar consideration may be given to the erosion produced by droplets. Since the surface of the drop is curved, the model cannot strictly be applied because the contact point is decelerating; however, if it is assumed that, at any instant when the contact angle is β , the above model gives, in the vicinity of the contact point, the value of pressure for a rigid surface or deformation velocity for a plastic surface, then the distribution of pressure or normal velocity can be calculated. The model then predicts a pressure or normal velocity corresponding to β equal to zero at the impact centre; both of these increase towards the edge of the impact as β increases. They reach a maximum when β becomes large enough for shock detachment and the subsequent jetting to occur. Pressure distributions of this type have been observed experimentally by Brunton & Rochester (1979) and calculated using a more accurate method by Lesser (1979). The former have found pressures around $\rho_0 c_0 v$ at the impact centre, rising to $2.5\rho_0 c_0 v$ at the edge of the impact, where the figures have been corrected to an impact on a rigid surface. The edge pressure agrees quite closely with the pressure produced at shock detachment (19).

For the plastic surface, the deformation velocity will be a maximum at shock detachment, but the time available for deformation will be a maximum at the centre of the impact. Therefore, in general the pit depth will not necessarily be a maximum at the centre, and, as mentioned previously, calculation of the exact pit profile will require more detailed treatment of the plastic flow.

The present model idealizes the response of the material as rigid-perfectly plastic, implying that the impact is communicated instantaneously to the whole material volume and that there is no plastic wave propagated into the material. These

assumptions can only be justified on grounds of simplicity to aid understanding in the first instance; considering an elastic–perfectly plastic material is the next step logically. Indeed this has already been alluded to in discussion of the establishment of plastic flow either immediately behind the elastic ‘precursor’ wave or after the passage of a release wave in the solid. It can be shown that one of the main effects of incorporating elasticity is to increase the threshold velocity v_0 by $p_Y/\rho_m c_m$, where ρ_m and c_m are the density and bulk sound speed respectively of the solid material. For the aluminium considered here, this increase amounts to about 24 m/s, i.e. about 11 %. Another effect occurs if the contact point is moving supersonically with respect to the solid material. In this case the large-scale plastic deformation cannot be established until a release wave has been propagated in the solid; consequently there is less time available for deformation to occur. The conditions when this is important lie below the sonic line shown in figure 8; the effect is mostly confined to the very small angles and high impact velocities.

A further step to make the model more realistic is to adopt an elastic–plastic material with a bilinear stress–strain curve. In this case the gradient of the plastic part of the curve gives the speed of propagation of the plastic wave. If this is known then the pressure and deformation velocity produced by the impact can be calculated. Preliminary calculations indicate that the deformation velocity is reduced by about 50 % when the effective specific acoustic impedance of the plastic material, i.e. material density times plastic wave speed, approaches that of the liquid. Also, in this case, the plastic deformation will not cease immediately on passage of the release wave but when the stress has been reduced to the yield stress.

5. Conclusions

The above analysis of normal and oblique shocks in liquid (water) has been used to extend Bowden & Brunton’s (1961) model of the impact of a plane-ended liquid mass and Heymann’s (1969) model of the impact of a wedge-shaped liquid mass on a rigid surface to the impact on a perfectly plastic surface. The results confirm that of Heymann and of Field *et al.* (1979) for the case of impact on a rigid surface by showing that, for a plane-ended impact, the pressure produced is somewhat in excess of the linear ‘water-hammer’ pressure because of the increase in liquid bulk modulus; for the wedge-shaped impact it was confirmed that the impact pressure is increased as shock detachment is approached reaching a value of about three times the ‘water-hammer’ pressure.

If the solid is perfectly plastic and it is assumed that the large-scale plastic deformation is immediately established in the impact zone, then for the plane-ended case the model predicts a threshold impact velocity below which no deformation can occur. When this is exceeded the rate of deformation is constant, and, if the impacting liquid mass is cylindrical, the maximum depth of pit, produced at the centre of the impact, is proportional to the cylinder radius and the excess of impact velocity over the threshold velocity. The threshold velocity depends upon the stress required to produce full-scale plastic flow, which is effectively the hardness of the material. The threshold impact velocities for normal engineering materials are rather large, possibly outside the range that would normally be encountered in, for example, cavitation-bubble microjets.

This difficulty with the model can be resolved by considering a wedge-shaped liquid mass, for which the rate of deformation increases as shock detachment is approached. When this occurs, the shock is at right-angles to the oncoming flow, viewed in a

reference frame fixed to the contact point. There is now no threshold velocity, and deformation can occur at any impact velocity provided that the wedge angle has a suitable value. For the impact of a cylindrical mass with a conical tip, the maximum possible depth, corresponding to shock detachment, occurs at the centre of the impact and is directly proportional to cylinder radius and impact velocity. This depth diminishes with increasing plastic flow stress. The model can possibly be used to find the pit geometries for the impact of microjets, associated with cavitation bubbles, and spherical droplets on a perfectly plastic surface.

REFERENCES

- BATCHELOR, G. K. 1967 *An Introduction to Fluid Dynamics*. Cambridge University Press.
- BOWDEN, F. P. & BRUNTON, J. H. 1961 The deformation of solids by liquid impact at supersonic speeds. *Proc. R. Soc. Lond. A* **263**, 433–450.
- BOWDEN, F. P. & FIELD, J. E. 1964 The brittle fracture of solids by liquid impact, by solid impact and by shock. *Proc. R. Soc. Lond. A* **282**, 331–352.
- BRUNTON, J. H. & ROCHESTER, M. C. 1979 Erosion of solid surfaces by impact of liquid drops. *Treatise on Materials Science and Technology* vol. 16 (ed. C. M. Preece), pp. 185–248. Academic.
- FIELD, J. E., LESSER, M. B. & DAVIES, P. N. H. 1979 Theoretical and experimental studies of two-dimensional liquid impact. In *Proc. 5th Intl Conf. on Erosion by Liquid and Solid Impact, Cambridge, 1979*.
- HEYMANN, F. J. 1969 High speed impact between a liquid drop and a solid surface. *J. Appl. Phys.* **40**, 5113–5122.
- LESSER, M. B. 1979 The fluid mechanics of liquid drop impact with rigid surfaces. In *Proc. 5th Intl Conf. on Erosion by Liquid and Solid Impact, Cambridge, 1979*.
- LESSER, M. B. 1981 Analytic solutions of liquid-drop impact problems. *Proc. R. Soc. Lond. A* **377**, 289–308.
- LUSH, P. A. 1979 Surface deformation produced by a cavitating flow. In *Proc. 5th Intl Conf. on Erosion by Liquid and Solid Impact, Cambridge, 1979*.
- PLESSET, M. S. & CHAPMAN, R. B. 1971 Collapse of an initially spherical vapour cavity in the neighbourhood of a solid boundary. *J. Fluid Mech.* **47**, 238–290.
- TABOR, D. 1951 *The Hardness of Metals*. Oxford University Press.